Binding of π-Acceptor Ligands to (Triamine)iron(II) Complexes

Andrew C. Moreland and Thomas B. Rauchfuss*

School of Chemical Sciences, University of Illinois, Urbana, Illinois 61801

Received October 26, 1999

A series of $(Me_3TACN)Fe^{II}$ derivatives with soft coligands have been investigated, where Me_3TACN is *N*,*N*′,*N*″-trimethyl-1,4,7-triazacyclononane. Treatment of Me_3TACN with $FeCl_2$ afforded a compound with the empirical formula $(Me_3TACN)FeCl_2$ (**1**). Compound **1**, which is a versatile precursor reagent, was shown by single-crystal X-ray diffraction to be the salt $[(Me_3TACN)_2Fe_2Cl_3][(Me_3TACN)FeCl_3]$, containing isolated $[(Me_3TACN)_2Fe_2Cl_3]^+$ and $[(Me_3TACN)FeCl_3]^-$ subunits. Treatment of **1** with $NaBPh_4$ gave the known $[(Me_3TACN)_2Fe_2Cl_3]BPh_4$, while the addition of Me_3TACN to $FeCl_4^{2-}$ gave $[(Me_3TACN)FeCl_3]^-$. Oxygenation of **1** afforded $[(Me_3TACN)FeCl_2]_2(\mu\text{-O})$, which was shown crystallographically to be centrosymmetric with a pair of distorted octahedral Fe centers. The Fe−N bond trans to the Fe−O bond is elongated by 0.2 Å relative to the other Fe−N distances. Solutions of **1** and thiolates absorb CO to give $[(Me_3TACN)Fe(SPh)(CO)_2]BPh_4$ and $(Me_3TACN)Fe(S_2C_2H_4)(CO)$ ($\nu_{CO} = 1896$ cm^{-1}). Treatment of **1** with excess CN^- afforded $[(Me_3TACN)Fe(CN)_3]^-$, isolated as its PPh_4^+ salt **5**. Crystallographic and spectroscopic studies show that **5** is low spin with a C_{3v} structure; its Fe−N distances contracted by 0.23 Å relative to those in $[(Me_3TACN)FeCl_3]^-$. Aqueous solutions of **1** bind CO upon the addition of CN^- to produce $(Me_3TACN)Fe(CN)_2(CO)$ (**6**). Analogous to **6** is $(Me_3TACN)Fe(CN)_2(CNMe)$, prepared by methylation of **5**. The metastable dicarbonyl $[(Me_3TACN)FeI(CO)_2]I$ was prepared by treatment of $FeI_2(CO)_4$ with Me_3TACN and was crystallographically characterized as its BPh_4^- salt. Values of $E_{1/2}$ for $[(Me_3TACN)FeCl_3]^-$, **5**, and **6** are −0.409, −0.640, and 0.533 V vs Fc/Fc^+, respectively.

Introduction

Recent years have witnessed increased interest in the binding of π-acid ligands to metal centers bearing classical ligands such as amines. To some extent, this theme is rooted in very old chemistry. Copper and ruthenium ammine complexes of π-acid ligands have been fruitfully investigated since the 1960s.[1−3] Ruthenium−ammine chemistry cannot be extended to Fe compounds because the $Fe^{II}-NH_3$ linkage is typically labile.

In this investigation of the ligand-binding properties of amine−Fe^{II} centers, we have focused on the R_3TACN family of facially coordinating tridentate ligands, where TACN is 1,4,7-triazacyclononane and Me_3TACN is the bulkier *N*,*N*′*N*″-trimethyl derivative thereof.[4,5] The R_3TACN class of facially coordinating amine ligands has been employed extensively to probe the role of metal centers in biological systems. TACN complexes have proven particularly useful in the characterization of metals involved in dioxygen activation, as illustrated by the studies of Wieghardt[3,4] and Tolman.[5,6] These successes are due to the kinetic resilience of the $M-R_3TACN$ interaction as well as to the highly basic nature of the mesocyclic ligand. In contrast to unidentate NH_3−Fe derivatives, the $Fe(R_3TACN)$ fragment is robust and tolerates the introduction of diverse and reactive coligands. For example, our first foray into (TACN)Fe chemistry uncovered the exceptional species $(TACN)_2Fe_2(S_2)_3$,[7] the bonding and reactivity of which demonstrated the potential of the (TACN)Fe unit as a π-donor center.

We were especially interested in the ability of the R_3TACN−Fe system to support CO coligands. Studies of non-heme Fe−CO compounds provide insights into the electronic features that allow one to bind still more challenging substrates to Fe, such as N_2 and alkenes, as implicated in Fe-catalyzed nitrogen fixation and alkene polymerization catalysis,[8] respectively. It is now known that Fe^{II}−CO complexes are common to all metallohydrogenases;[9−11] thus expertise with Fe^{II}−CO systems should guide the preparation of active-site analogues. Other enzymes featuring non-heme Fe centers with soft donor ligands (thiolates, cyanide) include nitrile hydratase[12,13] and possibly nitrogenase.[14]

The binding of CO to amine−Fe^{II} complexes has been of intermittent interest since the 1970s. Noteworthy early results are those of Karlin and Lippard[15] and Markó et al.,[16] who isolated $Fe[SC_2H_4N(Me)C_2H_4N(Me)C_2H_4S](CO)_2$ and $Fe(SPh)_2$-

(1) Taube, H. *Pure Appl. Chem.* **1979**, *51*, 901−12.
(2) Hidai, M.; Mizobe, Y. *Chem. Rev.* **1995**, *95*, 1115−33.
(3) Schneider, R.; Jüstel, T.; Wieghardt, K.; Nuber, B. *Z. Naturforsch.* **1994**, *49B*, 330.
(4) Chaudhuri, P.; Wieghardt, K. *Prog. Inorg. Chem.* **1988**, *35*, 329−436.
(5) Halfen, J. A.; Tolman, W. B. *Inorg. Synth.* **1998**, *32*, 75−81.
(6) Halfen, J. A.; Mahapatra, S.; Wilkinson, E. C.; Kaderli, S.; Young, V. G.; Que, L.; Zuberbuhler, A. D.; Tolman, W. B. *Science* **1996**, *271*, 1397−400.
(7) Moreland, A. C.; Rauchfuss, T. B. *J. Am. Chem. Soc.* **1998**, *120*, 9376−7.
(8) Britovsek, G. J. P.; Gibson, V. C.; Kimberley, B. S.; Maddox, P. J.; McTavish, S. J.; Solan, G. A.; White, A. J. P.; Williams, D. J. *Chem. Commun.* **1998**, 849−50.
(9) Thauer, R. K.; Klein, A. R.; Hartmann, G. C. *Chem. Rev.* **1996**, *96*, 3031−42.
(10) Peters, J. W.; Lanzilotta, W. N.; Lemon, B. J.; Seefeldt, L. C. *Science* **1998**, *282*, 1853−8.
(11) Cammack, R. *Nature* **1999**, *397*, 214−5.
(12) Nagashima, S.; Nakasako, M.; Dohmae, N.; Tsujimura, M.; Takio, K.; Odaka, M.; Yohda, M.; Kamiya, N.; Endo, I. *Nature Struct. Biol.* **1998**, *5*, 347−52.
(13) Marlin, D. S.; Olmstead, M. M.; Mascharak, P. K. *Inorg. Chem.* **1999**, *38*, 3258−60.
(14) Burgess, B. K.; Lowe, D. J. *Chem. Rev.* **1996**, *96*, 2983−3011.
(15) Karlin, K. D.; Lippard, S. J. *J. Am. Chem. Soc.* **1976**, *98*, 6951−7.
(16) Takács, J.; Soós, E.; Nagy-Magos, Z.; Markó, L.; Gervasio, G.; Hoffmann, T. *Inorg. Chim. Acta* **1989**, *166*, 39−46.

10.1021/ic9912629 CCC: $19.00
Published on Web 06/16/2000

Scheme 1

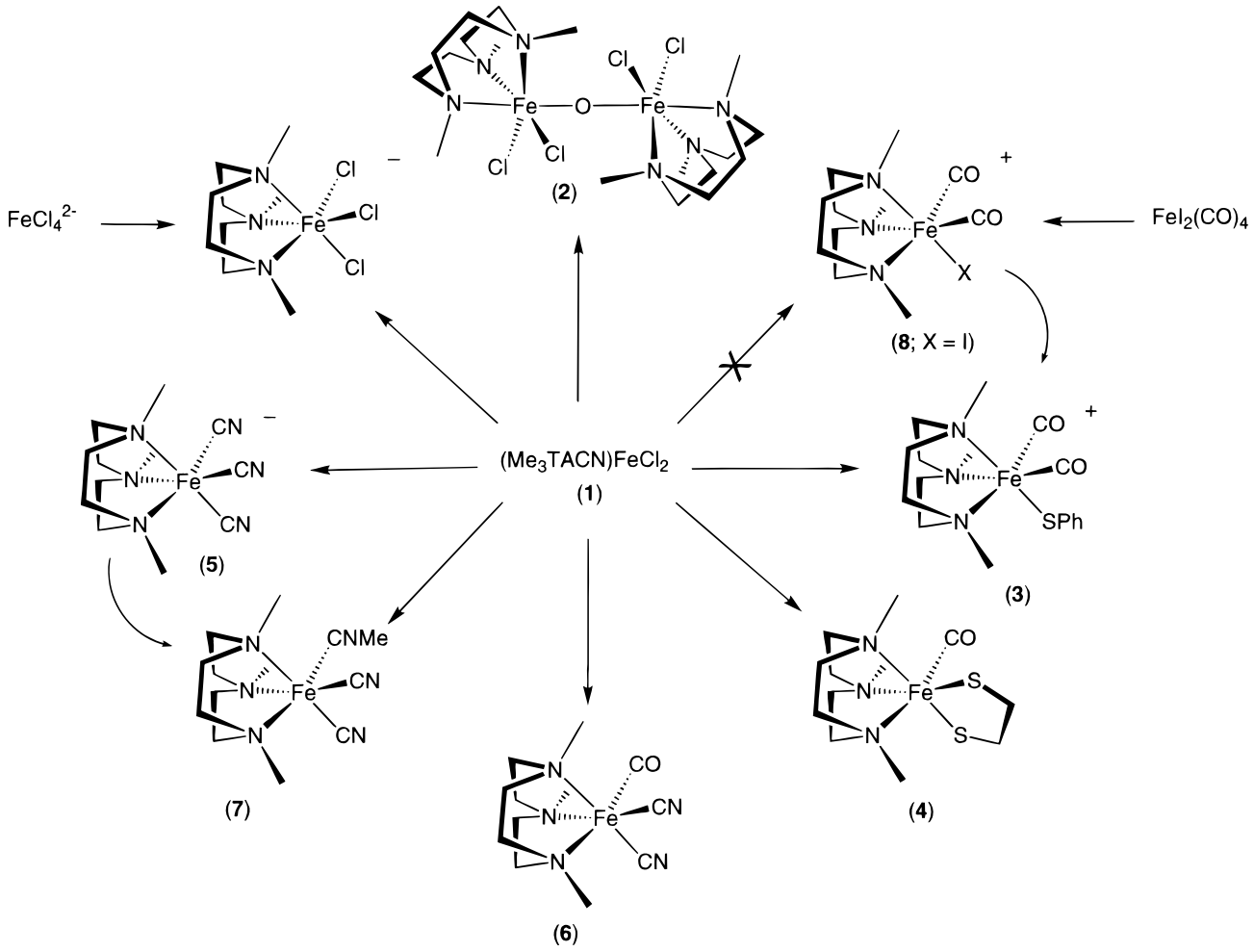

$(CO)_2$(en), respectively. Study of Fe−amine−CO species has been reinvigorated in recent years.[17−23] For example, in pursuing the relationship between the electronic structure and catalytic mechanism of nitrile hydratase,[17,24] Kovacs has reported the CO adduct of an Fe(diimino−amino−dithiolato) species. In contrast to the known amine−Fe^{II}−CO complexes, well-characterized $Fe^{II}N_2$ complexes all feature tertiary phosphine coligands.[25−30]

The principal compounds prepared in this project are summarized in Scheme 1.

Results

The principal precursor to the new $(Me_3TACN)Fe^{II}$ compounds results from the treatment of Me_3TACN with $FeCl_2$. This reaction afforded a tan solid analyzed as $(Me_3TACN)FeCl_2$ (**1**). Crystals grown from MeCN/Et_2O were examined by X-ray diffraction and shown to be the salt $[(Me_3TACN)_2Fe_2(\mu\text{-}Cl)_3^+][(Me_3TACN)FeCl_3^-]$ (eq 1). The cation $[(Me_3TACN)_2Fe_2(\mu\text{-}Cl)_3]^+$ was previously characterized by Wieghardt et al. as its BPh_4^- derivative (Figure 1).[31] This is a face-sharing bioctahedral species with a nonbonding Fe···Fe separation of 3.008 Å. The metrical details for the cation in **1** (see Table 1) are virtually identical to those of the BPh_4^- salt.[31] The anion $[FeCl_3(Me_3TACN)]^-$ is new. This species has idealized C_{3v} symmetry. The Fe−Cl distances in the anion (2.4467(9)−

$$3FeCl_2 + 3Me_3TACN \rightarrow [(Me_3TACN)_2Fe_2(\mu\text{-}Cl)_3^+][(Me_3TACN)FeCl_3^-] \quad (1)$$

(17) Ellison, J. J.; Nienstedt, A.; Shoner, S. C.; Barnhart, D.; Cowen, J. A.; Kovacs, J. A. *J. Am. Chem. Soc.* **1998**, *120*, 5691−700.
(18) Sellmann, D.; Mahr, G.; Knoch, F.; Moll, M. *Inorg. Chim. Acta* **1994**, *224*, 45−59.
(19) Sellmann, D.; Sutter, J. *Acc. Chem. Res.* **1997**, *30*, 460−9. Sellmann, D. *New J. Chem.* **1997**, *21*, 681−9.
(20) Davies, S. C.; Hughes, D. L.; Richards, R. L.; Sanders, J. R. *Chem. Commun.* **1998**, 2699−700. Davies, S. C.; Evans, D. J.; Hughes, D. L.; Longhurst, S.; Sanders, J. R. *Chem. Commun.* **1999**, 1935−6.
(21) Hsu, H.-F.; Koch, S. A.; Popescu, C. V.; Münck, E. *J. Am. Chem. Soc.* **1997**, *119*, 8371−2.
(22) Mauro, A. E.; Casagrande, O. L., Jr.; Nogueira, V. M.; Santos, R. H. A.; Gambardella, M. T. P.; Lechat, J. R.; Filho, M. F. J. *Polyhedron* **1993**, *12*, 297−301.
(23) Liaw, W.-F.; Chen, C.-H.; Lee, G.-H.; Peng, S.-M. *Organometallics* **1998**, *17*, 2370−2372.
(24) Marini, P. J.; Murray, K. S.; West, B. O. *J. Chem. Soc., Dalton Trans.* **1983**, 143−51.
(25) Hills, A.; Hughes, D. L.; Jimenez-Tenorio, M.; Leigh, G. J.; Rowley, A. T. *J. Chem. Soc., Dalton Trans.* **1993**, 3041−9.
(26) Ghilardi, C. A.; Midollini, S.; Sacconi, L.; Stoppioni, P. *J. Organomet. Chem.* **1981**, *205*, C193−202.
(27) Hughes, D. L.; Leigh, J.; Jimenez-Tenorio, M.; Rowley, A. T. *J. Chem. Soc., Dalton Trans.* **1993**, 75−82.
(28) Wiesler, B. E.; Lehnert, N.; Tuczek, F.; Neuhausen, J.; Tremel, W. *Angew. Chem., Int. Ed. Engl.* **1998**, *37*, 815−6.
(29) Buys, I. E.; Field, L. D.; Hambley, T. W.; McQueen, A. E. D. *Acta Crystallogr.* **1993**, *C49*, 1056−9.
(30) de la J. Leal, A.; Jiménez-Tenorio, M.; Puerta, M. C.; Valerga, P. *Organometallics* **1995**, *14*, 3839−47.
(31) Bossek, U.; Nühlen, D.; Bill, E.; Glaser, T.; Krebs, C.; Weyhermüller, T.; Wieghardt, K.; Lengen, M.; Trautwein, A. X. *Inorg. Chem.* **1997**, *36*, 2834−43.

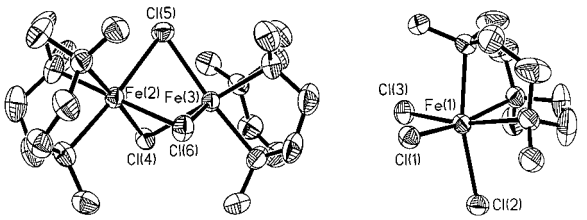

Figure 1. Structures of the anion and cation in "$(Me_3TACN)FeCl_2$" (**1**), with thermal ellipsoids drawn at the 50% level.

Table 1. Selected Bond Distances (Å) and Angles (deg) for **1**

Fe(1)−N(1)	2.307(3)	Fe(2)−Cl(6)	2.4729(9)
Fe(1)−N(2)	2.321(3)	Fe(2)−Cl(5)	2.4921(9)
Fe(1)−N(3)	2.327(3)	Fe(2)−Cl(4)	2.5197(9)
Fe(1)−Cl(3)	2.4467(9)	Fe(3)−N(9)	2.193(3)
Fe(1)−Cl(1)	2.4486(9)	Fe(3)−N(8)	2.194(3)
Fe(1)−Cl(2)	2.4589(9)	Fe(3)−N(7)	2.210(3)
Fe(2)−N(6)	2.197(3)	Fe(3)−Cl(5)	2.4820(9)
Fe(2)−N(4)	2.212(3)	Fe(3)−Cl(4)	2.4913(9)
Fe(2)−N(5)	2.207(3)	Fe(3)−Cl(6)	2.5129(9)
Cl(3)−Fe(1)−Cl(1)	97.67(3)	Cl(5)−Fe(3)−Cl(6)	87.25(3)
Cl(3)−Fe(1)−Cl(2)	97.94(3)	Cl(4)−Fe(3)−Cl(6)	87.60(3)
Cl(1)−Fe(1)−Cl(2)	97.27(3)	Fe(3)−Cl(4)−Fe(2)	73.77(3)
Cl(6)−Fe(2)−Cl(4)	87.85(3)	Fe(3)−Cl(5)−Fe(2)	74.41(2)
Cl(5)−Fe(2)−Cl(4)	86.56(3)	Fe(2)−Cl(6)−Fe(3)	74.40(3)

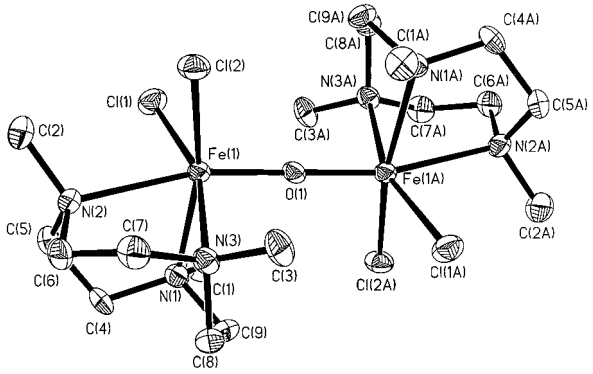

Figure 2. Structure of $[(Me_3TACN)FeCl_2]_2(\mu\text{-O})$ (**2**), with thermal ellipsoids drawn at the 50% level.

2.4589(9) Å) are significantly longer than those in $(Me_3TACN)Fe^{III}Cl_3$ (2.300(1)−2.309(1) Å).[32] The Fe−N distances are also elongated, but less dramatically so: 2.307(3)−2.327(3) Å for Fe^{II} vs 2.232(2)−2.264(2) Å for Fe^{III}.[32] When compared to those of other $Fe^{II}(Me_3TACN)$ species, for example, $[(Me_3TACN)Fe(NCS)_2]_2$ (2.25(1)−2.27(2) Å),[33] the Fe−N distances are slightly longer as well, perhaps due to the effect of negative charge. Acetonitrile solutions of **1** exhibit a conductivity of 133 Ω^{-1} cm^{-1}, which is independent of concentration over the range 0.50−5.0 mM.

The ^{1}H NMR spectrum of **1** shows five signals in MeCN solution. Three of these signals are assigned to $[(Me_3TACN)_2Fe_2Cl_3]^+$, as seen for an independently prepared sample (see below). One of these three signals has double the expected intensity and is the result of accidental degeneracy. One of the coincidental signals and the other two signals are assigned to the anion $[(Me_3TACN)FeCl_3]^-$. In CD_3OD solution, all six signals are resolved. Treatment of methanolic solutions of **1** with $NaBPh_4$ afforded a 77% yield of $[(Me_3TACN)_2Fe_2Cl_3]BPh_4$, thus confirming the relationship of **1** to Wieghardt's derivative. The facility and efficiency of this conversion suggest that the Cl^- ligands in $[(Me_3TACN)FeCl_3]^-$ are kinetically labile. We were unable to convert **1** into $PPh_4[(Me_3TACN)FeCl_3]$ by the reaction of **1** with an excess of PPh_4Cl. On the other hand, the observation of $[(Me_3TACN)FeCl_3]^-$ in solutions of **1** shows that the anion is not spontaneously unstable with respect to the dinuclear cation, implying that the nonreaction of Cl^- and $[(Me_3TACN)_2Fe_2Cl_3]^+$ is due to kinetic factors, e.g., slow cleavage of the $Fe(\mu\text{-}Cl)_3Fe$ bridge. ^{1}H NMR analysis did confirm that $(PPh_4)_2[FeCl_4]$ and Me_3TACN react to give exclusively $[(Me_3TACN)FeCl_3]^-$ (Chart 1). Interestingly, D_2O solutions of **1** feature only three signals, suggesting a rather simple structure.

Table 2. Selected Bond Distances (Å) and Angles (deg) for **2**

Fe(1)−O(1)	1.8190(7)	Fe(1)−N(3)	2.258(4)
Fe(1)−N(1)	2.237(4)	Fe(1)−Cl(1)	2.3426(15)
Fe(1)−N(2)	2.414(4)	Fe(1)−Cl(2)	2.3789(14)
O(1)−Fe(1)−N(1)	92.98(11)	N(3)−Fe(1)−Cl(2)	88.88(11)
O(1)−Fe(1)−N(3)	97.91(11)	Cl(1)−Fe(1)−Cl(2)	93.25(5)
N(1)−Fe(1)−N(3)	78.56(15)	O(1)−Fe(1)−N(2)	167.28(11)
O(1)−Fe(1)−Cl(1)	100.68(4)	N(1)−Fe(1)−N(2)	75.34(15)
N(1)−Fe(1)−Cl(1)	94.21(11)	N(3)−Fe(1)−N(2)	75.14(15)
N(3)−Fe(1)−Cl(1)	160.39(11)	Cl(1)−Fe(1)−N(2)	85.42(11)
O(1)−Fe(1)−N(1)	92.98(11)	Cl(2)−Fe(1)−N(2)	88.47(11)
O(1)−Fe(1)−N(3)	97.91(11)	Fe(1)−O(1)−Fe(1)#1	180.00(5)

Chart 1. Equilibria Related to the $(Me_3TACN)Fe^{II}$−Cl System

$$2LFeCl_2 \rightleftharpoons [L_2Fe_2Cl_3]^+ + [LFeCl_3]^-$$

$$2[LFeCl_3]^- \leftrightarrows [L_2Fe_2Cl_3] + 3Cl^-$$

$$3NaBPh_4 + 2[LFeCl_3]^- \rightleftharpoons [L_2Fe_2Cl_3^+]BPh_4^- + 2NaCl + 2BPh_4^-$$

$$[FeCl_4]^{2-} + L \rightarrow [LFeCl_3]^- + Cl^-$$

The cyclic voltammograms of solutions of **1** showed a reversible event at −0.409 V vs Fc^+/Fc, which is not present in solutions of $[(Me_3TACN)_2Fe_2Cl_3]BPh_4$. This redox process, which is a reduction, is assigned to the $[(Me_3TACN)FeCl_3]^{0/-}$ couple. This assignment was confirmed by electrochemical measurements on independently prepared $(Me_3TACN)FeCl_3$.[34]

Aerobic oxidation of solutions of **1** afforded orange crystals of $[(Me_3TACN)FeCl_2]_2(\mu\text{-O})$ (**2**). The new compound is soluble in water and only slightly soluble in polar organic solvents such as MeOH and MeCN. Like other high-spin d^5 complexes, such as $(Me_3TACN)FeCl_3$, compound **2** exhibits no detectable ^{1}H NMR spectrum.

Compound **2** was further characterized by single-crystal X-ray diffraction. The complex is described as a corner-shared bioctahedral species, each Fe center being held in an OCl_2N_3 coordination sphere. The Fe−O−Fe angle is constrained at 180° by the crystallographically imposed centrosymmetry (Figure 2, Table 2). A similar compound, $[(Me_3TACN)Fe(acac)]_2(\mu\text{-O})(ClO_4)_2$, which has no crystallographically imposed symmetry, has an Fe−O−Fe angle of 158.6(3)°.[35] In both compounds, the Fe−N bond trans to oxygen is longer than the other metal−ligand distances. In **2**, the length of the Fe−N bond trans to Fe−O is 2.414(4) Å and the cis Fe−N distances are 2.237(4)−2.258(4) Å, while in $[(Me_3TACN)Fe(acac)]_2(\mu\text{-O})(ClO_4)_2$, the Fe−N distances are 2.161(6) and 2.229(6) Å for the bonds cis

(32) Silver, G. C.; Trogler, W. C. *J. Am. Chem. Soc.* **1995**, *117*, 3983−93.
(33) Pohl, K.; Wieghardt, K.; Nuber, B.; Weiss, J. *J. Chem. Soc., Dalton Trans.* **1987**, 187.
(34) Chaudhuri, P.; Winter, M.; Wieghardt, K.; Gehring, S.; Haase, W.; Nuber, B.; Weiss, J. *Inorg. Chem.* **1988**, *27*, 1564−9.
(35) Wieghardt, K.; Pohl, K.; Bossek, U.; Nuber, B.; Weiss, J. *Z. Naturforsch.* **1988**, *43B*, 1184−94.

Table 3. Selected IR and ^{1}H NMR Data (Obtained in CH_3CN or CD_3CN Solutions)

compound	ν_{CX} (cm^{-1})	δ_{Me} (rel intens)
[(Me$_3$TACN)Fe(SPh)(CO)$_2$]BPh$_4$ (**3**)	2040	3.29 (2)
	1988	2.88 (1)
(Me$_3$TACN)Fe(S$_2$C$_2$H$_4$)(CO) (**4**)	1896	3.33 (1)
		2.61 (2)
PPh$_4$[(Me$_3$TACN)Fe(CN)$_3$] (**5**)	2052	2.99 (3)
	2035	
(Me$_3$TACN)Fe(CN)$_2$CO (**6**)	2097	3.35 (1)
	2092	2.92 (2)
	1960	
(Me$_3$TACN)Fe(CN)$_2$(CNMe) (**7**)	2131	3.56 (1, CNMe)
	2068	3.30 (1)
	2037	2.96 (2)
[(Me$_3$TACN)FeI(CO)$_2$]BPh$_4$ (**8**)	2051	3.55 (2)
		2.85 (1)

and trans to the terminal oxo ligand, the overall contraction of Fe−N distances in the cationic species being attributable to electrostatic effects. The Fe−Cl distances in **2** are 2.3789(14) and 2.3426(15) Å, which are slightly longer than those in (Me$_3$TACN)FeCl$_3$ (2.300(1)−2.309(1) Å).[32] Also related to **2** is the mixed-valence anion [(Me$_3$TACN)Fe(dbm)]$_2$(μ-O)$^-$ (dbm is the β-ketoenolate dibenzoylmethanide).[36] In this case, the Fe−N distances are for N trans to oxide 0.1 Å longer than the other Fe−N distances.

(Me$_3$TACN)Fe−SR−CO Derivatives. Compound **1** is a useful precursor to the series (Me$_3$TACN)Fe−SR−CO, which allowed us to assess the influence of thiolato ligands on CO binding. The simple derivative [(Me$_3$TACN)Fe(SPh)(CO)$_2$]$^+$ was generated by treatment of a methanolic solution of **1** with NaSPh to afford a brown intermediate, which was not further characterized. This solution absorbed CO gas to give a red derivative, which was isolated by precipitation as its BPh_4^- salt. The new compound, [(Me$_3$TACN)Fe(SPh)(CO)$_2$]BPh$_4$ (**3**), was isolated in ∼75% yield. ^{1}H NMR spectroscopic characterization indicates that **3** is a diamagnetic species with an Me resonance pattern consistent with the C_s symmetry. As will be illustrated for other compounds discussed below, the chemical shifts for the NMe groups trans to CO are observed in the region δ 3.25−3.55 (Table 3). The IR spectrum of **3** in the CO region exhibits two intense signals at 2040 and 1988 cm^{-1}. The CO ligands in **3** were not displaced by an N_2 purge, unlike the situation for [(Me$_3$TACN)FeI(CO)$_2$]$^+$ (see below). We obtained **3** even when the reaction was conducted with a 2-fold excess of PhSNa: (Me$_3$TACN)Fe(SPh)$_2$(CO) was not observed (see contrasting situation for (Me$_3$TACN)Fe(CN)$_2$(CO), below).

To investigate the influence of two thiolato ligands on the CO-binding properties of the Fe^{II} center, we undertook the synthesis of an ethanedithiolato derivative of **1**. A solution of **1** was treated with methanolic $Na_2S_2C_2H_4$ followed by CO to give a red-violet species. The product, (Me$_3$TACN)Fe(S$_2$C$_2$H$_4$)(CO) (**4**), was purified by extraction into CH_2Cl_2 followed by precipitation with Et_2O. The NMR data indicate that **4** is diamagnetic with C_s symmetry. The IR spectrum shows that ν_{CO} = 1896 cm^{-1}, more than 100 cm^{-1} lower frequency than the average of the ν_{CO} bands for **3**.

[(Me$_3$TACN)Fe(CN)$_3$]$^-$. The simple tricyano derivative [(Me$_3$TACN)Fe(CN)$_3$]$^-$ was readily prepared by treatment of a methanolic solution of **1** with slightly greater than three equiv of KCN. Addition of PPh_4Cl to the reaction mixture afforded orange microcrystals of PPh$_4$[(Me$_3$TACN)Fe(CN)$_3$] (**5**) in excellent yield. The NMR and IR spectra for this species are unexceptional and fully consistent with the C_{3v} symmetry. Microanalysis indicates that the product crystallizes as the monohydrate. The ^{13}CN-labeled complex was prepared similarly using K^{13}CN. The isotopic shift for ν_{CN} in the infrared spectrum is 44 cm^{-1} (2052 and 2035 cm^{-1} for ^{12}CN; 2008 and 1991 cm^{-1} for ^{13}CN).

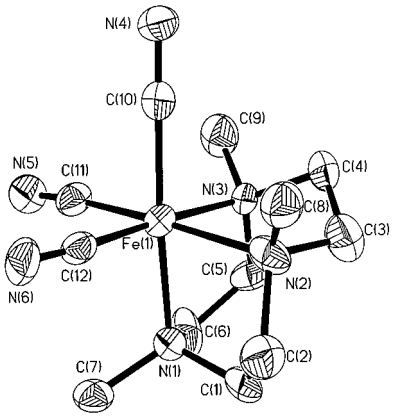

Figure 3. Structure of the anion [(Me$_3$TACN)Fe(CN)$_3$]$^-$ in **5**, with thermal ellipsoids drawn at the 50% level.

Table 4. Selected Bond Distances (Å) and Angles (deg) for **5**

Fe(1)−C(11)	1.868(9)	Fe(1)−N(1)	2.089(4)
Fe(1)−C(12)	1.877(9)	C(10)−N(4)	1.169(7)
Fe(1)−C(10)	1.882(6)	C(11)−N(5)	1.175(10)
Fe(1)−N(2)	2.082(6)	C(12)−N(6)	1.174(10)
Fe(1)−N(3)	2.087(6)		
C(11)−Fe(1)−C(12)	90.6(3)	N(2)−Fe(1)-N(3)	84.2(2)
C(11)−Fe(1)−C(10)	89.5(4)	C(11)−Fe(1)−N(1)	92.1(5)
C(12)−Fe(1)−C(10)	89.0(4)	C(12)−Fe(1)−N(1)	95.3(4)
C(11)−Fe(1)−N(2)	175.1(6)	C(10)−Fe(1)−N(1)	175.4(3)
C(12)−Fe(1)−N(2)	92.2(7)	N(2)−Fe(1)−N(1)	83.7(2)
C(10)−Fe(1)−N(2)	94.5(3)	N(3)−Fe(1)−N(1)	82.9(2)
C(11)−Fe(1)−N(3)	92.9(7)	N(4)−C(10)−Fe(1)	179.3(7)
C(12)−Fe(1)−N(3)	176.1(7)	N(5)−C(11)−Fe(1)	172(2)
C(10)−Fe(1)−N(3)	92.7(3)	N(6)−C(12)−Fe(1)	176.0(17)

Cyclic voltammetry studies demonstrate that the potential of the couple [(Me$_3$TACN)Fe(CN)$_3$]$^{0/-}$ occurs at −0.640 V vs Fc/Fc$^+$ in MeCN. For comparison, the redox potential of [Fe(CN)$_6$]$^{4-/3-}$ is −0.921 V vs Fc$^+$/Fc in MeCN. However, the ferrocyanide potential can vary by >1 V depending on solvent, with values of +0.079 V in H_2O to −0.971 V in DMF.[37] A similar compound, [Fe(CN)$_4$(diamine)]$^{-/2-}$ has an $E_{1/2}$ value of +0.058 V in H_2O,[38−40] which is closer to that of aqueous [Fe(CN)$_6$]$^{3-/4-}$, but solvent effects were not investigated for this diamine derivative. The effect of solvent on the redox potential for **5** was evaluated. The potentials of the redox couple, [(Me$_3$TACN)-Fe(CN)$_3$]$^{0/-}$, are −0.240 V in H_2O, −0.297 V in MeOH, and −0.640 V in MeCN, all vs Fc/Fc$^+$. The trend of redox potential increase reflects the fact that polar, hydrogen-bonding solvents stabilize the ferrous state. This trend is similar to that seen for ferrocyanide but less dramatic.

X-ray crystallographic analysis of **5** revealed that Fe is octahedral in an N_3C_3 coordination sphere (Figure 3, Table 4). The Fe−N distances in **5** (2.082(6)−2.089(4) Å) are dramatically shorter than those in high-spin Fe^{II}(Me$_3$TACN) com-

(36) Müller, M.; Bill, E.; Weyhermüller, T.; Wieghardt, K. *Chem. Commun.* **1997**, 705−6.

(37) Mascharak, P. K. *Inorg. Chem.* **1986**, *25*, 245−7.
(38) Goto, M.; Takeshita, M.; Kanda, N.; Sakai, T.; Goedken, V. L. *Inorg. Chem.* **1985**, *24*, 582−7.
(39) Goedken, V. L. *J. Chem. Soc., Chem. Commun.* **1972**, 207−8.
(40) Kuroda, Y.; Tanaka, N.; Goto, M.; Sakai, T. *Inorg. Chem.* **1989**, *28*, 2163−9.

plexes: the Fe−N distances in $[(Me_3TACN)FeCl_3]^-$ (average 2.32 Å) are >0.2 Å longer than those in **5**. The Fe−CN distances in **5** (1.868(9)−1.882(6) Å) are slightly shorter than those in $[Fe(CN)_6]^{4-}$ (1.896(6)−1.909(6) Å).[41] Other Fe−CN−amine complexes have been known for many years, e.g., $[Fe(CN)_4(en)]^{2-}$, but have not been subject to structural studies.[39,40] Known examples of complexes with the basic formula $(TACN)M(CN)_3$ include those for M = Cr[42] and Co.[43]

$(Me_3TACN)Fe(CN)_2(CO)$. The preparation of the mixed CO−CN^- derivative $(Me_3TACN)Fe(CN)_2(CO)$ (**6**) was modeled on the procedure used for the thiolato carbonyl **3**. The synthesis of **6** proved, however, to be particularly challenging. Carbonylation of solutions of **1** in the presence of 2 equiv of Et_4NCN indeed generated CO-containing products, but it was difficult to purify the products because of the comparable solubilities of Et_4NCl, Et_4NCN, and **6**. An improved method for the preparation of **6** involved the reaction of aqueous **1** with 2 equiv of KCN under an atmosphere of CO (eq 2).

$$(Me_3TACN)FeCl_2 + 2CN^- + CO \rightarrow (Me_3TACN)Fe(CN)_2(CO) + 2Cl^- \quad (2)$$

The crude product contained **6** together with some **5** as well as other unidentified species. Charge-neutral **6** was purified by extraction into CH_2Cl_2; evaporation of this solution gave an orange solid that was spectroscopically and analytically pure. In this synthesis, CO intercepts intermediate cyano species, perhaps oligomers with μ-CN ligands.[44] Characterization of **6** relied on its straightforward and informative IR and NMR properties (Table 1). The ^{1}H NMR data confirm the C_s symmetry, and the shift patterns are consistent with one NMe group trans to CO and two NMe groups trans to CN. Solid samples of **6** are stable under a nitrogen atmosphere. Cyclic voltammetry studies show that **6** undergoes quasi-reversible oxidation at the relatively high potential of 0.533 V vs Fc/Fc^+. This can be compared with the value of −0.640 V for $[(Me_3TACN)Fe(CN)_3]^{0/-}$, as discussed above.

We investigated the possible carbonylation of **5** as a possible route to **6**. IR spectroscopic measurements show that MeCN solutions of **5** rapidly react with CO gas at room temperature to afford a small amount of a new complex with ν_{CO} = 2023, 1994 cm^{-1}. The identity of these new bands as ν_{CO} was confirmed by the carbonylation of $[(Me_3TACN)Fe(^{13}CN)_3]^-$, which produced the same IR signature as that of the new species. Using **6** as a standard for the relative intensities of ν_{CN} and ν_{CO}, the concentration of the new species was estimated to be ≤10% of the total Fe concentration. Note that signals for **6** were not observed. Upon evaporation, these carbonylated solutions yielded spectroscopically pure **5**, indicating that the CO is kinetically labile. It has been known for some years that $[Fe(CN)_6]^{4-}$ can be carbonylated at high pressures to give $[Fe(CN)_5(CO)]^{3-}$.[45]

The isocyanide analogue of **6** was prepared by exploiting the nucleophilic character of the FeCN units in **5**. Thus $(Me_3TACN)Fe(CN)_2(CNMe)$ (**7**) was obtained by addition of the methylating agent MeOTf to an MeCN solution of **5**. ^{1}H NMR measurements indicate that **7** has C_s symmetry, and the infrared spectrum shows three ν_{CN} bands assigned respectively to cyano (2068, 2037 cm^{-1}) and isocyano ligands (2131 cm^{-1}).

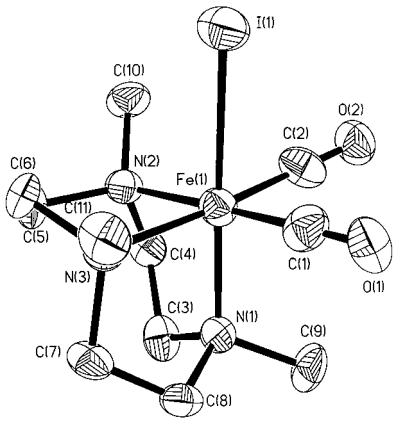

Figure 4. Structure of the cation $[(Me_3TACN)FeI(CO)_2]^+$ in **8**, with thermal ellipsoids drawn at the 35% level.

Table 5. Selected Bond Distance (Å) and Angles (deg) for **8**

I(1)−Fe(1)	2.6509(10)	Fe(1)−N(3)	2.069(5)
Fe(1)−C(1)	1.791(9)	Fe(1)−N(2)	2.072(5)
Fe(1)−C(2)	1.792(9)	O(1)−C(1)	1.146(9)
Fe(1)−N(1)	2.028(5)	O(2)−C(2)	1.133(8)
C(1)−Fe(1)−C(2)	89.6(3)	N(1)−Fe(1)−N(2)	84.4(2)
C(1)−Fe(1)−N(1)	94.7(3)	N(3)−Fe(1)−N(2)	84.2(2)
C(2)−Fe(1)−N(1)	95.9(3)	C(1)−Fe(1)−I(1)	83.1(2)
C(1)−Fe(1)−N(3)	93.9(3)	C(2)−Fe(1)−I(1)	83.9(2)
C(2)−Fe(1)−N(3)	176.3(3)	N(1)−Fe(1)−I(1)	177.76(15)
N(1)−Fe(1)−N(3)	85.2(2)	N(3)−Fe(1)−I(1)	95.19(14)
C(1)−Fe(1)−N(2)	178.0(3)	N(2)−Fe(1)−I(1)	97.79(13)
C(2)−Fe(1)−N(2)	92.3(3)	N(1)−Fe(1)−N(2)	84.4(2)

$[(Me_3TACN)FeI(CO)_2]^+$. An alternative route to $(Me_3TACN)Fe-CO$ complexes involved the reaction of $Fe(CO)_4I_2$ with Me_3TACN. Vigorous CO evolution occurred as the red-violet precursor was converted to pink $[(Me_3TACN)FeI(CO)_2]I$ (eq 3). The ^{1}H NMR spectrum of this salt shows the expected

$$FeI_2(CO)_4 + Me_3TACN \rightarrow [(Me_3TACN)FeI(CO)_2]I + 2CO \quad (3)$$

2:1 pattern for the NMe groups, the more intense signal being at δ 3.55, consistent with methyl trans to CO. The IR spectrum also indicates a dicarbonyl with a pair of ν_{CO} bands (2051, 2003 cm^{-1}), which are of ∼15 cm^{-1} higher energy than those of the analogous $(SPh)(CO)_2$ species **3**. In contrast to those in the other carbonyl complexes prepared in this work, the CO ligands in this species are labile, although the complex is stable under a CO atmosphere. The loss of CO is accompanied by a bleaching of the solution color. The progress of decarbonylation can be observed by UV−vis spectroscopy, monitoring the decrease in intensity of the bands at 338 and 512 nm. The change obeys isobestic behavior, and the kinetics are approximately first order ($k = 5.68 \times 10^{-4}$ s^{-1}, $t_{1/2}$ = 1220 s at 22 °C).

Treatment of methanolic $[(Me_3TACN)FeI(CO)_2]I$ with $NaBPh_4$ precipitated pink $[(Me_3TACN)FeI(CO)_2]BPh_4$ (**8**). Crystallographic analysis reveals an octahedral species (Figure 4, Table 5). The $FeI(CO)_2$ unit resembles that in $(C_5Me_5)FeI(CO)_2$,[46] e.g., in the Fe−I distances (2.6509(10) Å for Me_3TACN vs 2.6077(9) Å for the Cp* compound) and Fe−CO distances (1.792(9) Å for Me_3TACN vs 1.774(5) Å for the Cp* compound). In both

(41) Meyer, H.-J.; Pickardt, J. *Z. Anorg. Allg. Chem.* **1988**, *560*, 185−90.
(42) Kirk, A. D.; Namasivayam, C. *Inorg. Chem.* **1988**, *27*, 1095−9.
(43) Heinrich, J. L.; Berseth, P. A.; Long, J. R. *Chem. Commun.* **1998**, 1231−2.
(44) Vahrenkamp, H.; Geiss, A.; Richardson, G. N. *J. Chem. Soc., Dalton Trans.* **1997**, 3643−51.
(45) Cotton, F. A.; Monchamp, R. R.; Henry, R. J. M.; Young, R. C. *J. Inorg. Nucl. Chem.* **1959**, *10*, 28.
(46) Akita, M.; Terada, M.; Tanaka, M.; Moro-Oka, Y. *J. Organomet. Chem.* **1996**, *510*, 255−61.

cases, the bond distances are slightly longer for the Me_3TACN compound, perhaps as a consequence of steric crowding. The Fe−N distances are, on average, slightly shorter still than those in the other low-spin Fe^{II} compound, **5** (averages: 2.056(5) vs 2.086(6) Å for **5**). The Fe−N distance trans to I is 0.04 Å shorter than the Fe−N distances trans to CO. Qualitative experiments confirm that **8** can be converted to the other carbonyl complexes **3** and **6** by treatment with SPh^- and CN^-, respectively.

Discussion

In our investigation of CO derivatives of the amine−Fe^{II} systems, we have focused on the Me_3TACN derivatives for reasons of stoichiometric control: less bulky triamines, e.g., TACN itself, often form complexes of the type $Fe(triamine)_2^{n+}$, which are unsuitable for ligand substitution.[47] An additional reason for using Me_3TACN instead of TACN is that unmethylated $(TACN)FeCl_3$ is very poorly soluble. A drawback of the high basicity of Me_3TACN, however, is the stabilization of ionic derivatives such as $[(Me_3TACN)_2Fe_2(\mu\text{-}Cl)_3^+][(Me_3TACN)FeCl_3^-]$ (**1**), not simple monomeric or dimeric derivatives, $[(Me_3TACN)FeCl_2]_x$. We had hoped to obtain $[(Me_3TACN)FeCl_2]_2$, which would serve as an analogue of such well-known species as $[(ring)MCl_2]_2$ (where (ring)M = (arene)Ru and $(C_5Me_5)Rh$). Nonetheless, compound **1** generally behaves as an equivalent of $(Me_3TACN)FeCl_2$ and appears to be versatile, even beyond the immediate theme of amine−Fe−CO compounds. We note that Wieghardt has in fact reported $[(Me_3TACN)FeX_2]_2$ (X^- = NCO^-, SCN^-).[33]

Parallel to studies on **1**, we examined the synthetic utility of the "precarbonylated" species $[(Me_3TACN)FeI(CO)_2]I$, which is prepared from the readily available $FeI_2(CO)_4$. The inability of **1** to bind CO is consistent with the tendency of $[(Me_3TACN)FeI(CO)_2]^+$ to expel CO. The important and relatively subtle role of the coligand L in controlling the π-basicity of $[(Me_3TACN)FeL_n]^+$ ($n \leq 2$; L = I^-, CN^-, SPh^-) is demonstrated by the binding of CO to thiolato and cyanido derivatives of **1**.

All metallohydrogenases feature $Fe(CN)_n(CO)$ units as part of a bimetallic active site.[11] This fact led us to examine Me_3TACN−Fe−CO−CN derivatives in order to learn more about the electronic characteristics of this subunit and to elucidate some facts that may ultimately be relevant to the biosynthesis of the Fe−CN−CO subunit. The desired $(Me_3TACN)Fe(CN)_2(CO)$ compound was prepared via two routes: (i) treatment of $[(Me_3TACN)FeI(CO)_2]^+$ with CN^- and (ii) treatment of "$(Me_3TACN)FeCl_2$" sources with CN^- under an atmosphere of CO. The latter method presumably involves the carbonylation of an intermediate dicyano derivative. Previous examples of $L_nFe(CN)_2(CO)$ species are the cyclopentadienyl derivatives $[(C_5R_5)Fe(CN)_2(CO)]^-$. In selected solvents, IR spectra of $[(C_5R_5)Fe(CN)_2(CO)]^-$ match those of the hydrogenase enzymes in the ν_{CO} and ν_{CN} regions.[48,49] Koch[21] has reported related complexes of the type $Fe(PR_3)(SR)_3(CO)(CN)^{2-}$. Our principal observation on the Me_3TACN−Fe−CO−CN system is that CO binding to Fe^{II} is enhanced by the presence of CN^- coligands relative to halide coligands. This enhancement indicates the synergy arising from the strong donor properties of the CN^- ligands that stabilize the π-interaction between Fe^{II} and CO. This view is supported by trends in the vibrational data (see Table 1).

It is also significant that $(Me_3TACN)Fe(CN)_2(CO)$ is susceptible to oxidation, albeit at the relatively high potential of 0.533 V vs Fc^+/Fc. Very few $Fe^{II}CO$ complexes undergo chemically reversible oxidation, as summarized by Koch, who described a complex of the type $Fe^{III}(CN)(SR)_3(PR_3)(CO)^{2-}$. The shift in potential of ~1.2 V for $[(Me_3TACN)Fe(CN)_2(CO)]^{+/0}$ vs $[(Me_3TACN)Fe(CN)_3]^{0/-}$ is substantial. Though some of the change in redox potential can be attributed to charge effects, a large part of the 1.2 V shift is attributed to the differing donor properties of CO and CN^-. On the basis of the ν_{CO} bands for the complexes reported in this work, it is clear that electron-rich iron complexes can be generated using classical ligand sets.

Similarly, the lability of the CO correlates with the ν_{CO} values: the derivative with high values of ν_{CO} (i.e., $[(Me_3TACN)Fe(CO)_2I]^+$) is labile, while $(Me_3TACN)Fe(CN)_2(CO)$ and $(Me_3TACN)Fe(S_2C_2H_4)(CO)$ are stable with respect to the loss of CO. Kovacs has reported an iron complex which ν_{CO} value of ~1900 cm^{-1} but which is also labile;[17] however, this lability may reflect the ability of the coligand to adopt a trigonal bipyramidal coordination geometry after decarbonylation.

Experimental Section

Materials and Methods. Solvent purifications and spectroscopic measurements were conducted as previously described.[50] The following compounds were prepared using literature procedures: $FeCl_2$,[51] $FeI_2(CO)_4$,[52] and Me_3TACN.[4,53] All manipulations were carried out under an atmosphere of purified nitrogen using either Schlenk techniques or an inert-atmosphere glovebox. Redox potentials were measured relative to Ag/AgCl (saturated KCl) or $Ag/AgPF_6$ (0.1 M Bu_4NPF_6 in MeCN). The reported potentials are referenced to ferrocene by comparing the potential to $E_{1/2}$ of Fc measured under similar conditions (0.434 V vs Ag/AgCl, (saturated KCl), 0.115 V vs $Ag/AgPF_6$ (0.1 M Bu_4NPF_6 in MeCN)).

$[(Me_3TACN)_2Fe_2Cl_3][(Me_3TACN)FeCl_3]$ (1). A stirred slurry of 0.317 g (2.50 mmol) of anhydrous $FeCl_2$ in 20 mL of MeCN was treated with 0.50 mL (2.58 mmol) of Me_3TACN. After 2 h, the yellow solution was filtered to remove traces of unreacted $FeCl_2$. The filtrate was reduced in volume to 5 mL; addition of 50 mL of Et_2O precipitated the product. Yield: 0.664 g (89%). X-ray-quality crystals were grown by diffusion of Et_2O vapors into a MeCN solution of **1**. ^1H NMR (CD_3CN): δ 121.6 (12H, CH_2, cation), 103.2 (24H, Me, cation, and CH_2, anion), 53.2 (12H, CH_2, cation), 46.2 (9H, Me, anion), 39.7 (6H, CH_2, anion). ^1H NMR (CD_3OD): δ 122.3 (12H, CH_2, cation), 111.5 (6H, CH_2, anion), 103.6 (18H, Me, cation), 69.1 (12H, CH_2, cation), 53.1 (9H, Me, anion), 41.3 (6H, CH_2, anion). ^1H NMR (D_2O): δ 117.5 (6H, CH_2), 83.2 (9H, Me), 41.5 (6H, CH_2). Anal. Calcd for $C_{27}H_{63}N_9Cl_6Fe_3$ (found): C, 36.27 (36.08); H, 7.10 (7.13); N, 14.10 (13.94).

Solution Conductivity of $[(Me_3TACN)_2Fe_2Cl_3][(Me_3TACN)FeCl_3]$ (1). The solution conductivity was measured on 0.50−5.0 mM solutions of **1** in an inert-atmosphere glovebox, employing a model 31A conductance bridge and a model 3403 cell (cell constant k = 1.0/cm), both from Yellow Springs Instrument Co., Yellow Springs, OH.

In Situ Generation of $[(Me_3TACN)FeCl_3]^-$. A slurry of 6.0 mg (0.047 mmol) of $FeCl_2$ in 1 mL of CD_3CN was treated with 35 mg (0.093 mmol) of PPh_4Cl, and the mixture was stirred until all solids dissolved. The resulting solution of $(PPh_4)_2[FeCl_4]$[54] was treated with 9.0 μL (0.047 mmol) of Me_3TACN, and the ^1H NMR spectrum was recorded within minutes. ^1H NMR: δ 104.7 (6H, CH_2), 42.2 (9H, Me),

(47) Wu, L. P.; Yamagiwa, Y.; Ino, I.; Sugimoto, K.; Kuroda-Sowa, T.; Kamikawa, T.; Munakata, M. *Polyhedron* **1999**, *18*, 2047−53.
(48) Lai, C.-H.; Lee, W.-Z.; Miller, M. L.; Reibenspies, J. H.; Darensbourg, D. J.; Darensbourg, M. Y. *J. Am. Chem. Soc.* **1998**, *120*, 10103−14.
(49) Pierik, A. J.; Roseboom, W.; Happe, R. P.; Bagley, K. A.; Albracht, S. P. J. *J. Biol. Chem.* **1999**, *274*, 3331−7.
(50) Pafford, R. J.; Chou, J.-H.; Rauchfuss, T. B. *Inorg. Chem.* **1999**, *38*, 3779−86.
(51) Kovacic, P.; Brace, N. O. *Inorg. Synth.* **1960**, *6*, 172−3.
(52) Brunner, H.; Herrmann, W. A. *Anorganisch-Chemisches Praktikum für Fortgeschrittene: Metallorganische Chemie;* Fachbereich Chemie und Pharmazie, Universität Regensburg: Regensburg, Germany, 1979.
(53) Wieghardt, K.; Chaudhuri, P.; Nuber, B.; Weiss, J. *Inorg. Chem.* **1982**, *21*, 3086−90.
(54) Gill, N. S.; Taylor, F. B. *Inorg. Synth.* **1967**, *9*, 136−42.

39.0 (6H, CH_2). Attempts to generate $[(Me_3TACN)FeCl_3]^-$ by the addition of up to a 10-fold excess of PPh_4Cl to solutions of **1** in CD_3CN resulted in no reaction over the course of 24 h, as judged by ^1H NMR analysis.

$[(Me_3TACN)_2Fe_2Cl_3][BPh_4]$. To a solution of 50 mg **1** (0.056 mmol) in 5 mL of MeCN was added a stirred solution of $NaBPh_4$ (29 mg, 0.085 mmol) in 5 mL of MeCN. After 1 h, a white precipitate (NaCl) as well as a lightening in color was observed. The NaCl was removed by filtration, and the colorless product was precipitated from the filtrate by the addition of 50 mL of Et_2O. Yield: 58 mg (77%).

Alternatively, the product could be synthesized in higher purity by the addition of a solution of 80 mg (0.23 mmol) of $NaBPh_4$ in 5 mL of MeOH to a solution of 62 mg (0.21 mmol) of **1** in 5 mL of MeOH. The product precipitated in analytical purity. Yield: 72 mg (78%). ^1H NMR (CD_3CN): δ 121.6 (12H, CH_2), 103.2 (18H, Me), 53.2 (12H, CH_2), 7.27 (8H, BPh_4), 6.99 (8H, BPh_4), 6.83 (4H, BPh_4). Anal. Calcd for $C_{42}H_{62}N_6BCl_3Fe_2$ (found): C, 57.33 (57.32); H, 7.10 (6.97); N, 9.55 (9.47).

$[(Me_3TACN)FeCl_2]_2(\mu$-O) (2). Dry O_2 was bubbled at a rate of ca. 5 bubbles/s into a solution of 50 mg (0.168 mmol) of **1** in 15 mL of MeCN. The solution color changed quickly from pale yellow to green, immediately followed by the precipitation of orange microcrystals. The reaction mixture was filtered, and the solid was washed with Et_2O. Yield: 25 mg (49%). The yield was low because of the partial solubility of the product in MeCN. Anal. Calcd for $C_{18}H_{42}N_6Cl_4Fe_2O$ (found): C, 35.32 (35.73); H, 6.92 (6.91); N, 13.73 (13.34).

$[(Me_3TACN)Fe(SPh)(CO)_2]BPh_4$ (3). A solution of NaOMe was prepared by dissolving 6.7 mg (0.17 mmol) of a 60% dispersion (hexane washed) of NaH in 20 mL of MeOH. To the NaOMe solution was added 17 μL (0.17 mmol) of PhSH, and the mixture was transferred via cannula to a solution of 50 mg (0.17 mmol) of **1** in 10 mL of MeOH. A color change to yellow-brown occurred. The homogeneous solution was treated with CO delivered through a needle at a rate of ~5 bubbles/s, and the color of the solution changed to red. After 15 min, the carbonylation was discontinued, and a solution of 68 mg (0.20 mmol) of $NaBPh_4$ in 10 mL of MeOH was added. The resulting brown precipitate was filtered off and washed with MeOH and Et_2O. Yield: 87 mg (72%). ^1H NMR (CD_3CN): δ 3.29 (6H, 2 Me), 2.88 (3H, Me), 3.27 (2H, CH_2), 3.12 (2H, CH_2), 3.05 (2H, CH_2), 2.95 (2H, CH_2), 2.84 (2H, CH_2), 2.77 (2H, CH_2), 7.53 (2H, SPh), 7.16 (2H, SPh), 7.26 (9H, SPh and BPh_4), 6.98 (8H, BPh_4), 6.83 (4H, BPh_4). IR (CH_3CN): 2040, 1988 cm^{-1}. Anal. Calcd for $C_{41}H_{46}N_3BFeO_2S\cdot 0.5MeOH$ (found): C, 68.51, (68.54); H, 6.65 (6.42); N, 5.78 (5.51).

$(Me_3TACN)Fe(S_2C_2H_4)(CO)$ (4). A solution of $Na_2(S_2C_2H_4)$ was prepared using 12 mg (0.31 mmol) of 60% NaH and 13 μL (0.15 mmol) of $HSCH_2CH_2SH$ in 10 mL of MeOH. This solution was transferred via cannula to a solution of 46 mg (0.15 mmol) of **1** in 5 mL of MeOH. The resulting pale red solution was purged with CO gas for 5 min, causing a color change to red-violet. The carbonylation was discontinued, and the solvent was removed in vacuo. The crude product was extracted into 5 mL of CH_2Cl_2, followed by filtration to remove NaCl. The product was precipitated from the filtrate by the addition of 30 mL of Et_2O and was washed with Et_2O. Yield: 38 mg (72%). ^1H NMR (CD_3CN): δ 3.33 (3H, Me), 2.61 (6H, 2 Me), 3.39 (2H, CH_2), 2.99 (2H, CH_2), 2.55 (8H, CH_2), 2.28 (2H, $S_2C_2H_4$), 1.84 (2H, $S_2C_2H_4$). IR (CH_3CN): 1896 cm^{-1}. Anal. Calcd for $C_{12}H_{25}N_3FeOS_2\cdot 0.3CH_2Cl_2$ (found): C, 39.63 (39.65); H, 6.92 (6.87); N, 11.27 (11.07).

$[PPh_4][(Me_3TACN)Fe(CN)_3]$ (5). A mixture of 0.200 g (0.67 mmol) of **1** and 0.219 g (3.36 mmol) of KCN was dissolved in 10 mL of MeOH. An immediate change occurred, giving a dark brown color, which lightened to orange over 2 h at 25 °C. The orange solution was treated with 0.252 g (0.67 mmol) of PPh_4Cl, resulting in partial precipitation of the product. The mixture was evaporated to dryness, and the resulting residue was extracted into 75 mL of CH_2Cl_2, followed by filtration through Celite to remove undissolved KCl and excess KCN. The CH_2Cl_2 solution was concentrated to 15 mL, and the product was precipitated as an orange solid by the addition of 100 mL of Et_2O. Yield: 0.314 g (73%). X-ray-quality crystals were grown by diffusion of Et_2O vapors into an MeCN solution of the product. ^1H NMR (CD_2Cl_2): δ 2.99 (9H, 3 Me), 2.95 (6H, CH_2), 2.51 (6H, CH_2), 7.95 (8H, PPh_4), 7.78 (8H, PPh_4), 7.64 (4H, PPh_4). IR (KBr): 2053, 2036 cm^{-1}. Anal. Calcd for $C_{36}H_{41}N_6FeP\cdot 0.5H_2O$ (found): C, 66.16 (66.01); H, 6.48 (6.20); N, 12.86 (12.27).

$(Me_3TACN)Fe(CN)_2(CO)$ (6). A solution of 81 mg (0.27 mmol) of **1** in 5 mL of CO-degassed H_2O was placed under a CO atmosphere. IR measurements indicated that no reaction had occurred. While CO was flowing through the apparatus, a solution of 27 mg (0.56 mmol) of NaCN in 5 mL of H_2O was added dropwise to give an orange solution, after which the solvent was removed in vacuo. Under an atmosphere of N_2, the crude product was extracted into 5 mL of CH_2Cl_2 and the undissolved NaCl was removed by filtration. A yellow-orange powder was precipitated by the addition of Et_2O. The product was filtered off, washed with Et_2O, and dried under N_2. Yield: 58 mg (69%). ^1H NMR (CD_3CN): δ 3.35 (3H, Me), 2.92 (6H, 2 Me), 3.54 (2H, CH_2), 2.96 (2H, CH_2), 2.87 (2H, CH_2), 2.70 (2H, CH_2), 2.53 (4H, CH_2). IR (CH_3CN): 2097, 2092 (ν_{CN}), 1960 (ν_{CO}) cm^{-1}. Anal. Calcd for $C_{12}H_{21}N_5FeO\cdot H_2O$ (found): C, 44.32 (44.20); H, 7.13 (7.11); N, 21.10 (21.54).

$(Me_3TACN)Fe(CN)_2(CNMe)$ (7). A solution of 63 mg (98 μmol) of $PPh_4[(Me_3TACN)Fe(CN)_3]$ in 15 mL of MeCN was treated with 11 μL (0.095 mmol) of MeO_3SCF_3. A color change from orange to yellow was observed. Solvent was removed in vacuo, and the residue was extracted into 5 mL of CH_2Cl_2. The product precipitated upon addition of Et_2O; the solid was filtered off, washed with Et_2O, and dried under N_2. No attempts were made to remove $PPh_4(O_3SCF_3)$, which coprecipitated with the product. ^1H NMR (CD_3CN): δ 3.56 (3H, CNMe), 3.30 (3H, NMe), 3.24 (2H, CH_2), 3.05 (2H, CH_2), 2.96 (6H, 2 NMe), 2.65 (8H, CH_2). IR (CH_3CN): 2131 (ν_{CNMe}), 2068, 2037 cm^{-1} (ν_{CN}).

$[(Me_3TACN)FeI(CO)_2]$I. To a solution of 0.660 g (1.57 mmol) of $FeI_2(CO)_4$ in 15 mL of CH_2Cl_2 was added 0.32 mL (1.64 mmol) of Me_3TACN. Vigorous CO evolution occurred as the red-violet solution turned brown and then pink. After 30 min, the product was precipitated from the homogeneous solution by the addition of 50 mL of Et_2O. Filtration followed by drying under nitrogen afforded a light red solid. Yield: 0.755 g (90%). ^1H NMR (CD_3CN): δ 3.55 (6H, 2 Me), 2.85 (3H, Me), 3.41 (4H, CH_2), 3.26 (4H, CH_2), 2.82 (2H, CH_2), 2.71 (2H, CH_2). IR (CH_3CN): 2051, 2003 cm^{-1}. Anal. Calcd for $C_{11}H_{21}N_3FeI_2O_2$ (found): C, 24.61 (24.95); H, 3.94 (4.22); N, 7.83 (8.17). A stirred solution of 82 mg (0.15 mmol) of $[(Me_3TACN)FeI(CO)_2]$I in 10 mL of MeCN was monitored by UV−vis spectroscopy. After 2 h at 25 °C, the solution had become colorless and the band at 512 nm had disappeared. The IR spectrum of the solution was featureless in the 1900−2200 cm^{-1} region. A solution of 0.122 g (0.227 mmol) of $[(Me_3TACN)FeI(CO)_2]$I in 5 mL of MeOH was treated with a solution of 0.120 g (0.346 mmol) of $NaBPh_4$ in 5 mL of MeOH. The pink precipitate (**8**) that formed immediately was filtered off and washed with MeOH and Et_2O. Yield: 0.132 g (80%). ^1H NMR (CD_3CN): δ 3.53 (6H, 2 Me), 2.83 (3H, Me), 3.39 (4H, CH_2), 3.20 (4H, CH_2), 2.84 (2H, CH_2), 2.69 (2H, CH_2), 7.27 (8H, BPh_4), 6.99 (8H, BPh_4), 6.84 (4H, BPh_4). IR (CH_3CN): 2051, 2003 cm^{-1}.

Crystallographic Analysis of $(C_9H_{21}N_3)_3Fe_3Cl_6\cdot CH_3CN$ (1). Colorless prismatic crystals of $(C_9H_{21}N_3)_3Fe_3Cl_6\cdot CH_3CN$ were grown from MeCN/Et_2O solutions at 25 °C. A crystal for analysis was attached to a thin glass fiber with Paratone-N oil (Exxon). The data crystal was bound by the $(00\bar{1})$, (001), $(11\bar{1})$, $(\bar{1}02)$, (011), $(0\bar{1}1)$, and $(01\bar{1})$ faces. Distances from the crystal center to these facial boundaries were 0.130, 0.130, 0.240, 0.200, 0.170, 0.140, and 0.170 mm, respectively. Data were collected at 198 K on a Siemens CCD diffractometer. Crystal and refinement details are given in Table 6. Systematic conditions suggested the unambiguous space group *Pbca*. The structure was solved by Direct Methods; correct positions for Cl, Fe, and N were deduced from an *E* map. Subsequent cycles of isotropic least-squares refinement followed by an unweighted difference Fourier synthesis revealed positions for all C atoms. H atom *U*'s were assigned as 1.2 times the U_{eq}'s of adjacent C atoms. Non-H atoms were refined with anisotropic thermal coefficients. Successful convergence of the full-matrix least-squares refinement of F^2 was indicated by the maximum shift/error for the last cycle.

Crystallographic Analysis of $[(C_9H_{21}N_3)Fe]_2O\cdot CH_2Cl_2$ (2). Orange needlelike crystals of $[(C_9H_{21}N_3)Fe]_2O\cdot CH_2Cl_2$ were grown from MeCN solutions at 22 °C. A crystal for analysis was attached to a thin glass fiber with Paratone-N oil (Exxon). The data crystal was bound by the

Table 6. Crystal Data and Structural Refinement Details for **1**, **2**, **5**, and **8**

	$(Me_3TACN)_3Fe_3Cl_6\cdot CH_3CN$ (**1**)	$[(Me_3TACN)FeCl_2]_2O\cdot CH_2Cl_2$ (**2**)	$PPh_4[(Me_3TACN)Fe(CN)_3]\cdot 0.5H_2O$ (**5**)	$[(Me_3TACN)FeI(CO)_2]BPh_4$ (**8**)
empirical formula	$C_{29}H_{66}Cl_6Fe_3N_{10}$	$C_{19}H_{44}Cl_6Fe_2N_6O$	$C_{36}H_{42}FeN_6O_{0.50}P$	$C_{35}H_{41}BFeIN_3O_2$
f w	935.17	694.99	653.58	729.27
crystal system	orthorhombic	orthorhombic	orthorhombic	monoclinic
space group	*Pbca*	*Pbcn*	*Imm*2	$P2_1/n$
a (Å)	12.1837(2)	13.8095(3)	20.7970(14)	10.3651(5)
b (Å)	21.4868(3)	13.5150(3)	22.6904(17)	21.0670(10)
c (Å)	34.1478(7)	16.0125(2)	7.1678(5)	15.0224(7)
α, β, γ, (deg)	90, 90, 90	90, 90, 90	90, 90, 90	90, 90.5540(10), 90
V (Å^3)	8939.5(3)	2988.50(10)	3382.4(4)	3280.2(3)
Z	8	4	4	4
ρ_{calc} (Mg m^{-3})	1.390	1.545	1.283	1.477
μ (mm^{-1})	1.352	1.532	0.529	1.436
T (K)	198(2)	198(2)	173(2)	193(2)
λ, Å	0.710 73	0.717 03	0.717 03	0.717 03
θ range for collcn (deg)	1.90−28.27	2.11−28.27	1.79−25.07	1.66−28.26
F(000)	3920	1440	1380	1488
no. of reflns collected	54 211	17 895	9076	21 473
no. of indep reflns (R_{int})[a]	10 835 (0.0433)[a]	3663 (0.1299)	3143 (0.0532)	21 473 (0.0814)
R index ($I > 2\sigma$)	0.0496	0.0666	0.0416	0.1163
R indices (all data): R1, wR2	0.0822, 0.1412	0.1257, 0.1975	0.0743, 0.0833	0.2300, 0.3506
crystal size (mm)	0.26 × 0.34 × 0.44	1.90 × 0.04 × 0.04	0.05 × 0.05 × 0.64	0.24 × 0.30 × 0.50
data/restraints/params	10 835/1/444	3663/0/156	3143/172/310	21 473/0/389
goodness of fit on F^2	0.948	1.141	1.115	2.043
largest peak and hole (e/Å^3)	1.094 and −0.618	0.780 and −0.551	0.284 and −0.300	4.070 and −2.001

[a] $R_{int} = \sum|F_o^2 - F_o^2(\text{mean})|/\sum F_o^2$.

($\bar{1}10$), ($1\bar{1}0$), (110), ($\bar{1}\bar{1}0$), (001), and ($00\bar{1}$) faces. Distances from the crystal center to these facial boundaries were 0.020, 0.020, 0.020, 0.020, 0.095, and 0.095 mm, respectively. Data were collected at 198 K on a Siemens CCD diffractometer. Crystal and refinement details are given in Table 6. Systematic conditions suggested the unambiguous space group *Pbcn*. The structure was solved by Direct Methods; correct positions for Cl, Fe, N, O, and C were deduced from an *E* map. H atom *U*'s were assigned as 1.2 times the U_{eq}'s of adjacent C atoms. Non-H atoms were refined with anisotropic thermal coefficients. Successful convergence of the full-matrix least-squares refinement of F^2 was indicated by the maximum shift/error for the last cycle.

Crystallographic Analysis of $Ph_4P[(C_9H_{21}N_3)Fe(CN)_3]\cdot 0.5H_2O$ (5). Yellow needlelike crystals of $Ph_4P[(C_9H_{21}N_3)Fe(CN)_3]\cdot 0.5H_2O$ were grown from MeCN/Et_2O solutions at 25 °C. A crystal for analysis was attached to a thin glass fiber with Paratone-N oil (Exxon). The data crystal was bound by the ($01\bar{1}$), ($0\bar{1}1$), (011), ($0\bar{1}\bar{1}$), (100), and ($\bar{1}00$) faces. Distances from the crystal center to these facial boundaries were 0.025, 0.025, 0.025, 0.025, 0.320, and 0.320 mm, respectively. Data were collected at 173 K on a Siemens CCD diffractometer. Crystal and refinement details are given in Table 6. Systematic conditions suggested the space group *Imm*2. The structure was solved by Direct Methods; correct positions for Fe, P, and N were deduced from an *E* map. Subsequent cycles of isotropic least-squares refinement followed by an unweighted difference Fourier synthesis revealed positions for all C atoms. H atom *U*'s were assigned as 1.2 times the U_{eq}'s of adjacent C atoms. Non-H atoms were refined with anisotropic thermal coefficients. Successful convergence of the full-matrix least-squares refinement of F^2 was indicated by the maximum shift/error for the last cycle.

Crystallographic Analysis of $[(C_9H_{21}N_3)FeI(CO)_2]BPh_4$ (8). Red prismatic crystals of $[(C_9H_{21}N_3)FeI(CO)_2]BPh_4$ were grown from MeCN/Et_2O solutions at −30 °C in the dark. A crystal for analysis was attached to a thin glass fiber with Paratone-N oil (Exxon). The data crystal was bound by the ($0\bar{1}0$), (010), (111), ($\bar{1}\bar{1}0$), ($0\ 0\bar{1}$), and ($11\bar{1}$) faces. Distances from the crystal center to these facial boundaries were 0.120, 0.120, 0.150, 0.200, 0.200, and 0.170 mm, respectively. Data were collected at 193 K on a Siemens CCD diffractometer. Crystal and refinement details are given in Table 6. Systematic conditions suggested the unambiguous space group $P2_1/n$. The best available crystals was severely twinned. The structure was solved by Direct Methods; correct positions for I, Fe, and B were deduced from a vector map. Subsequent cycles of isotropic least-squares refinement followed by an unweighted difference Fourier synthesis revealed positions for all N, O, and C atoms. H atom *U*'s were assigned as 1.2 times the U_{eq}'s of adjacent C atoms. Non-H atoms were refined with anisotropic thermal coefficients. Successful convergence of the full-matrix least-squares refinement of F^2 was indicated by the maximum shift/error for the last cycle. The highest residual electron density in the final difference Fourier map was in the vicinity of I(1). Efforts to model the twinning condition were unsuccessful.

Acknowledgment. This research was funded by the National Science Foundation and the U.S. Department of Energy.

Supporting Information Available: Listings of X-ray experimental details, atomic coordinates, bond distances and angles, and thermal parameters for compounds **1**, **2**, **5**, and **8**. This material is available free of charge via the Internet at http://pubs.acs.org.

IC9912629